Available online at www.sciencedirect.com

ScienceDirect

Procedia CIRP 98 (2021) 358–363

www.elsevier.com/locate/procedia

28th CIRP Conference on Life Cycle Engineering

Modeling energy and resource use in additive manufacturing of automotive series parts with multi-jet fusion and selective laser sintering

Mathias Wiese[a,b,*], Alexander Leiden[b], Christopher Rogall[b], Sebastian Thiede[b,c], Christoph Herrmann[b,d]

[a] *Polymer Additive Manufacturing Center, AUDI AG, Auto-Union-Straße 1, Ingolstadt, 85045, Germany*

[b] *Chair of Sustainable Manufacturing and Life Cycle Engineering, Institute of Machine Tools and Production Technology, Technische Universität Braunschweig, Langer Kamp 19b, Braunschweig, 38106, Germany*

[c] *Chair of Manufacturing Systems, Department Design, Production and Management, University of Twente, Drienerlolaan 5, Enschede, 7522NB, The Netherlands*

[d] *Fraunhofer Institute for Surface Engineering and Thin Films (IST), Bienroder Weg 54 E, Braunschweig, 38108, Germany*

Abstract

With additive manufacturing (AM) becoming a competitive manufacturing process for low to medium production volumes, rapid manufacturing becomes an increasingly relevant manufacturing approach. However, regulations and customers demand more eco-efficient life-cycles of products. This requires engineers and designers to pre-select between productive AM processes like selective laser sintering (SLS) and multi-jet fusion (MJF), based on their expected environmental impact in series production. As SLS already debuted in the mid-1980s, researches broadly explored parts' mechanical properties, energy and resource use. The multi-jet fusion (MJF) technology, introduced in 2017, delivers comparable part properties at considerably higher print speeds. However, its energy and resource use is still scarcely covered . To close this gap, this publication develops a model for evaluation of energy and resource utilization based on a case study with an automotive exterior series part using an EOS P396 SLS and a HP 4200 MJF machine. Data from measurements in energy and material consumption as well as the print job shows a good predictability and builds the basis for an environmental assessment. The derived model and its functional blocks allow estimation and comparison of sustainability for different use cases in rapid manufacturing with MJF and SLS. Despite the process similarities, results concerning greenhouse gas emissions and cumulative energy demand are different. The gained insights enhance pre-selection of manufacturing strategies, a suitable printing technology and the evaluation of AM processes during manufacturing according to sustainability aspects. Printer manufacturers and users may find this research insightful for improvements in sustainability and comparability of future AM processes.

Keywords: Rapid manufacturing; Energy efficiency; Resource efficiency; Additive manufacturing; Automotive engineering; Process modeling;

1. Introduction

New and more productive processes with improved material properties keep driving the advance of additive manufacturing (AM) into the domains of low to medium volume manufacturing and promise savings in time-to-market and lean supply chains [1–4]. The automotive industry is one of the main users of additive manufacturing [4, 5]. Among the available AM technologies and materials, processes like selective laser sintering (SLS) and the recently introduced multi-jet fusion (MJF) show high potential for applications in vehicle series production up to medium volumes. Though these productive thermoplastic-based processes are qualified to deliver end-use parts matching automotive quality criterions [1], they also need to align with corporate environmental targets and therefore be analyzed concerning their environmental impact. For a better understanding of the possibilities and contributions AM offers for a more sustainable manufacturing process of products, researchers recommend to foster understanding of its energy and material use. This especially applies when AM is used for end-use part manufacturing (rapid manufacturing) instead of prototyping applications, where a better understanding enhances decision making and process transparency for life cycle assessments [2, 6–9]. This paper contributes to this understanding by introducing

* Corresponding author. Tel.: +49 841 89987209
E-mail address: mathias.wiese@audi.de (Mathias Wiese).

2212-8271
10.1016/j.procir.2021.01.117

a model for energy and resource utilization in these two processes and applying it to a automotive series part case study.

2. Background

2.1. Fundamentals of SLS and MJF

SLS and MJF are members of the powder bed fusion (PBF) process family, which is characterized through the common mechanism of areas in a powder bed being fused selectively by heat energy [10]. They are especially qualified for the processing of semi-crystalline polymers such as Polyamide 12 (PA12) or Polyamide 11 (PA11), due to their well controllable melt behavior [11, 12]. Parts manufactured with these processes show comparable behavior in terms of mechanical, chemical, thermal, and dimensional properties [13–16], with MJF outperforming SLS in recyclability of unfused material [15].
However, significant process differences exist which are briefly addressed in the following, referring to Figure 1 and 2.

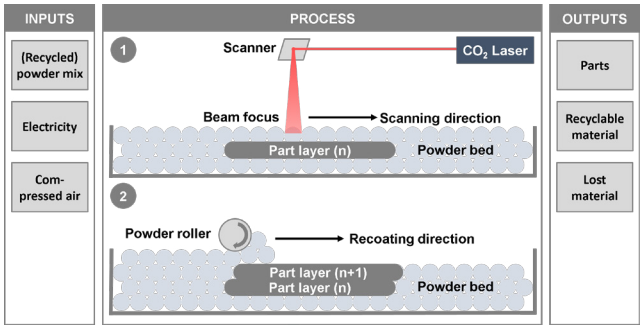

Fig. 1: Simplified functional principle of the SLS process

In the SLS process (Figure 1), the build chamber is maintained at a temperature just below the melting point of the powdered material. Preparing the build-up of a new layer in the recoating process, a thin layer of powder is spread across the build area and the existing part layer (n) using a counter-rotating powder leveling roller. The conditioned and pre-heated new layer is then selectively scanned by a focused CO_2 laser, fusing the powder particles of the respective cross section from a digital part model into a new part layer (n+1). This process is repeated until the build is completed [5, 17]. Overall process speed depends on the scanning speed, laser beam diameter and the cross section area of the different layers [5]. Unsintered material can be partially reused in a following build when new material is added in a reconditioning process [17].

While the recoating and build chamber conditioning of the MJF process (Figure 2) works in the same way as in the SLS process, the fusing mechanism is based on a different approach. MJF uses a combination of heat from an infrared lamp and agents for detailing and fusing applied by an inkjet printhead. During an overpass of the integrated heater and printhead array, it selectively deposits the fusing agent on the cross sections defining a part layer (n+1) in the powder bed. In addition to the fusing agent, a detailing agent is applied to the edge boundaries of cross sections infiltrated with fusing agent. This prevents coalescence bleed and improves the geometrical accuracy and surface quality of the fused layer. Following the agent deposition, the thermal energy from the infrared heater is transferred to the highly absorbent fusing agent, forming the new part layer [12, 18].

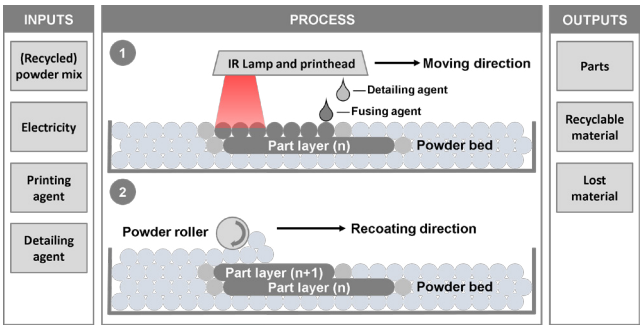

Fig. 2: Simplified functional principle of the MJF process

2.2. State of the art in understanding of energy and resource utilization of SLS and MJF

Since emergence of laser sintering, multiple researchers analyzed the energy and resource utilization in powder bed fusion processes. Sreenivasan and Bourell [19] performed a comprehensive analysis of the SLS process from an energy standpoint, tracking the energy demand of printer sub-systems like laser, heater, drives and peripheral equipment. Baumers et al. [20] extended energy analysis by assigning the print phases to mean power consumption, taking into account the geometry-dependencies, which related to less than 5.5% of total print power consumption. Highest dependencies were detected for general build time and Z-height of the print. On the lower end of energy use per kilogram of sintered material, Sreenivasan and Bourell [19] report 14.5 kwh/kg, whereas Baumers et al. [20] found values from 56 to 66 kwh/kg. Findings by Bertling et al. [21] and Kellens et al.[22, 23] also range between these boundaries. In addition to the impact of power consumption Kellens et al. [22] found waste material as a main contributor to SLS's environmental impact. Chen [2] reviews these implications and compares SLS to injection molding (IM) based parts' cumulative energy demand (CED) for raw materials and all subsequent production steps. Results found SLS to be competitive at very low production volumes. Tagliaferri et al. [24] conducted full life-cycle analysis of SLS and MJF, while making assumptions due to a lack of real printer energy consumption data and PA 12 material. These findings, the low data availability for the young MJF technology and similar potentials of SLS and MJF in part applications, imply the need for more accurate resource and energy modeling for these process alternatives. Especially when considering these technologies for small series manufacturing in future vehicle development, engineers need early predictions about the environmental impact of the product. This work addresses the mentioned research gaps by developing a modeling approach for energy and resource use in PBF systems, including first field data collection for the recently introduced MJF process.

2.3. Dynamic energy and resource flow simulation approaches

Simulation and modeling approaches in AM can be divided into process and system level applications. While the process level mainly focuses on interactions of material and process parameters within a machine, the system level analyses the behavior and interaction of machines in a manufacturing system. Regarding energy consumption and resource flow, Jackson et al. [25] developed a model to understand energy utilization in additive-substractive manufacturing for metallic tensile specimen. Yosofi et al. [26] developed a model for representation of the energy and resource flow in production with fused deposition modeling. Tagliaferri et al. [24] set up an environmental and economic analysis, but lack in-depth analysis of the machine characteristics. No approach is considering the specifics of the energy and resource demand for SLS and MJF processes, so a more specific simulation model is required. In manufacturing systems engineering, dynamic simulation aims for a representation of a system with its dynamic processes and their development over time in an experimentable environment in order to determine which can be transferred to reality [27]. Simulation approaches can be divided into four main paradigms: agent based (AB), discrete event (DE), dynamic system (DS) and system dynamics (SD) [28]. For 3D printers a combination of AB, DE and DS will be reasonable to model the energy and resource flows. The printer can be represented as agents in the simulation, while the printing process has a discrete character with defined machine states. The energy and resource demand are considered as dynamic development over time and therefore modeled as a DS. In the past various authors used these methods to model the energy and resource demand in different manufacturing systems. For example, Thiede developed a generic framework to model the energy demand of various manufacturing systems with a focus on exploring energy efficiency potentials [29]. These techniques will be applied to the methodology proposed in section 3.

3. Methodology

3.1. Dynamic energy and resource flow simulation approach for SLS and MJF

Based on a generic machine model, which can be found in various publications [29–32], a specific state-chart model has been derived for both AM technologies. A major difference to previous generic machine models is the consideration of the macro-perspective with the overall machine states (off, ramp-up, processing, idle) and the micro-perspective on the printing process itself, which consist of periodically reoccurring events like recoating and the passes for material fusing. As described in 2.2, energy consumption is mainly characterized by length and height of the print, implying a layer-based modeling approach in this micro-perspective. This way, print jobs with less height and duration can be modeled by scaling the printing phase as a function of the number of expected layers as shown in section 4. In the macro-perspective, the machine states apart from the print cycle are assumed to be independent of the build job characteristics. In addition to the mentioned components, periphery aggregates such as cooling units for the switch cabinet or laser systems can be modeled as separate system which is connected with the printer agent. After the printing process a post-printing phase can follow, for example to cool down the build unit of the printer.

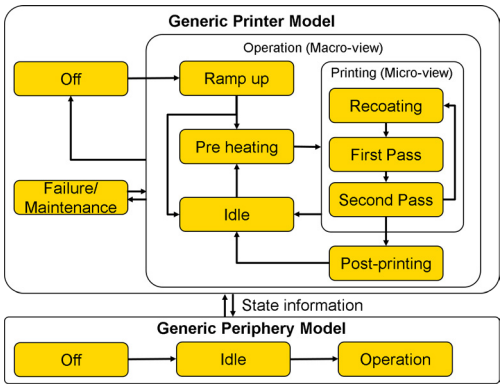

Fig. 3: Simplified machine state overview of the two PBF processes

Table 1: Equivalence factors for resource modeling

	Value	Unit	Source
PA12 CO_2-eq.	6.9	kg	[33]
PA12 primary energy	207	MJ/kg	[33]
Power (mix, Germany) CO_2-eq.	0.427	kg/kWh	[34]
MJF fusing agent CO_2-eq.	2.22	MJ/kg	[35]
MJF detailing agent CO_2-eq.	1.06	MJ/kg	[35]
MJF fusing agent primary energy	44.24	MJ/kg	[35]
MJF detailing agent primary energy	20.44	MJ/kg	[35]

To parametrize the model illustrated in Figure 3, energy and resource demand measurements and calculations are conducted for the production scenarios described in the following section. Resource modeling is based on the equivalence factors in Table 1 derived from local conditions and literature.

3.2. Production scenario definition for SLS and MJF

Energy and resource measurements are based on a case study of an automotive exterior trim part. Its geometrical dimensions and volume are well suited for efficient nesting and thus production through additive manufacturing. Based on this geometry, two production scenarios with one build job for each SLS and MJF machine were prepared using automated nesting routines. The first scenario aims for a production volume of n=145 parts on both machines, implying a full MJF build chamber and a partial build on the SLS machine which will be simulated by the parametrized model. The second scenario aims for production of n=250 parts, reflecting a full SLS build chamber and implying two builds on the MJF machine with n=145 and n=105 parts, which are subject to simulation. To parametrize the model, the fully nested build jobs were printed while energy and resource flows were monitored. Using the minimum distance settings in Table 2, the build jobs were optimized for

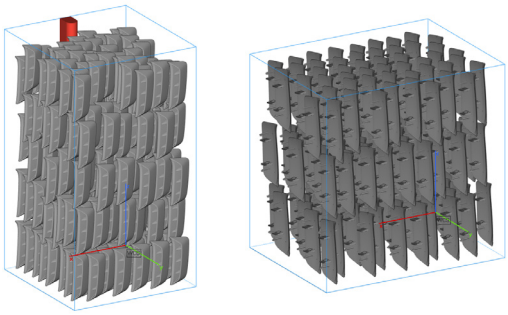

(a) EOS P396 (SLS; n=250) (b) HP 4210 (MJF; n=145)

Fig. 4: Fully nested build chambers for the parametrization prints on the SLS and MJF machine

maximum utilization while maintaining a similar packing density. This preparation led to the build job specifications in Table 2. Figure 4 depicts the two fully nested build chambers.

Table 2: Build job specifications and settings for the printed and simulated build jobs

	EOS P396 (SLS)	HP 4210 (MJF)	Unit
Measured & simulated full build jobs			
Print dimensions (x,y,z)	340 x 340 x 600	380 x 284 x 380	*mm*
Packing density	8.29	7.68	*%*
Number of parts	250	145	-
Total part volume	5420.33	3058.05	cm^3
Total part weight	4932.50	3133.02	*g*
Duration (incl. 1h idle)	1925	1090	*min*
Simulated partial build jobs			
Print dimensions (x,y,z)	340 x 340 x 366	380 x 284 x 273	*mm*
Packing density	7.91	7.72	*%*
Number of parts	145	105	-
Total part volume	3143.79	2268.74	cm^3
Total part weight	2860.85	2214.45	*g*
Duration (incl. 1h idle)	1249	827	*min*
Common parameters			
Min. part spacing	4	5	*mm*
Material	PA12	PA12	
Powder mix (new/reused)	50 / 50	20 / 80	*%*

Based on the full chamber prints, the model is then configured with the parametrization results presented in section 4.1 and applied to estimate resource and energy utilization in the two production scenarios.

4. Results for model parametrization and its application to energy and resource utilization in MJF and SLS

4.1. Model parametrization results

Based on the results from the real measurements, as shown in Figure 5, the parameters for the macro-perspective model

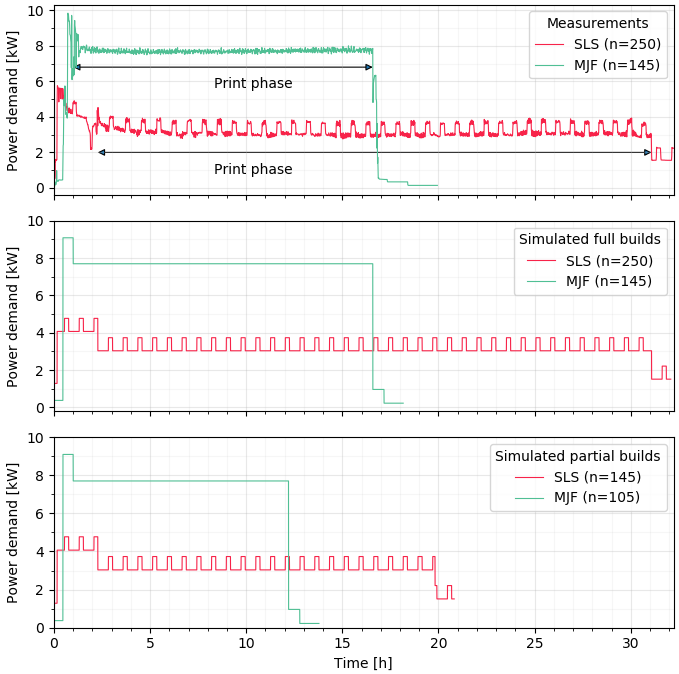

Fig. 5: Measured power demands and modeled power demands for the production scenarios with SLS and MJF

Table 3: Overview of average power demands and machine state durations during measurement

	EOS P396 (SLS)		HP 4210 (MJF)	
	P_{avg} $[kWh]$	t $[min]$	P_{avg} $[kWh]$	t $[min]$
System boot	1.284	10	0.373	28
Warm-up / Self-check	4.069	127	9.088	32
Printing	3.033	1728	7.697	935
Cyclic A/C	0.700	40x13	-	-
Cool-down	-	-	0.960	35
Idle	1.511	74	0.224	157
	P_{avg} $[Wh]$	t_{avg} $[s]$	P_{avg} $[Wh]$	t_{avg} $[s]$
Per printed layer*	17.43	20.70	23.67	11.07

*Avg. layer thickness: MJF=0.08 *mm*, SLS=0.12 *mm*

states are retrieved from the average power demands summarized in Table 3 in the different machine states. The measurements of power demand have been smoothed using PAA (piecewise aggregate approximation) with a window size of 45 seconds. Graphical comparison (see Table 3) of measured and modeled energy consumption shows a good fit of the model to the measurements. The average layer printing duration and energy demand parametrize the printing states as shown in Figure 3, enabling subsequent modeling of prints with less duration and height.

Table 4: Energy demand for production of a full print, single part and per kilogram of material

	SLS_{250}	SLS_{145}	MJF_{250}	MJF_{145}	Unit
Full print	103.4	67.3	217.7	125.7	*kWh*
Part (kg)	21.0	23.5	41.3	41.1	*kWh/kg*
Part (piece)	0.414	0.464	0.871	0.867	*kWh/pc*

4.2. *Resource and energy utilization results for the case study production scenarios*

After model parametrization and simulation of the build jobs from Table 4 the results for the two production scenarios show a diverse process performance. MJF consumes more than twice the energy per batch print and part. These findings point towards a significantly higher energy demand of the SLS process compared to MJF. Though great differences in energy use are found, further resources need to be incorporated into a holistic process comparison. Figure 6 and Figure 7 illustrate the cumulative energy demand (CED) respectively the global warming potential (GWP) per part calculated for the two scenarios.

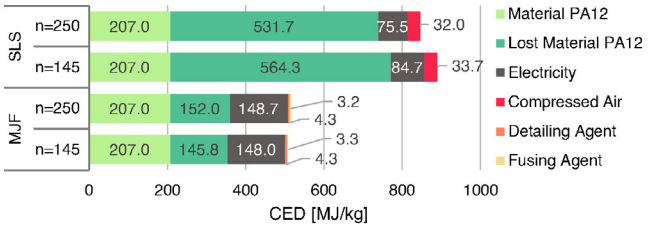

Fig. 6: Modeled CED per kilogram of part mass for n=145 and n=250 parts

The cumulative energy demand in Figure 6 shares a similar pattern with the global warming potential. Likewise to the GWP analysis, the material-related figures have the major influence on the energy demand. In this case SLS features 23-24% for part material and 63% of the energy demand in the domains of lost PA12 material, equalling more than 700 MJ/kg. The impact of higher material reusability in MJF is directly visible with comparably lower figures at around 40-41% of CED in final part material and just 29-30% for lost material, equalling about 350 MJ/kg. From material perspective, MJF utilizes less than half of the CED found in SLS. However, higher power consumption leads to 29% of overall CED in MJF at around 148 MJ/kg. In the SLS process, 9-10% of CED can be attributed to power consumption and 4% to compressed air. The impact of detailing and fusing agents in the MJF process is less than 1% in both cases. In total, SLS ranges from 846 to 890 MJ/kg, whereas MJF achieves 508 to 515 MJ/kg.

The comparison of the CO_2-equivalents per kilogram of produced parts shows strong dependence on material consumption respectively the recycling rate. In the SLS process, 17-18% of the emissions are attributable to PA12 part material, while 47% are caused by non-recyclable PA12 material lost in the process. The better recycling rate of the MJF process leads to comparatively lower figures around 23% for PA12 part material and 16-

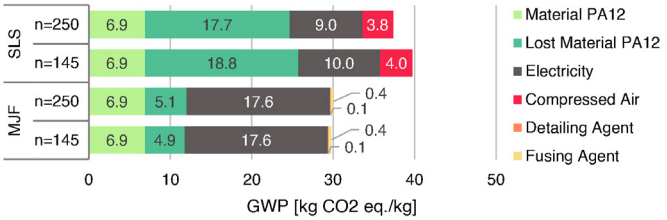

Fig. 7: Modeled GWP per kilogram of part mass for n=145 and n=250 parts

17% in lost material. Though it features lower material-related emissions, the MJF process suffers from high power consumption, causing 59% of the emissions with a total of 17.6 kg CO_2-eq, taking into account the local power mix (see Table 1. in both scenarios. This level exceeds the cumulative figure for compressed air and power consumption in the SLS process, which are contributing around 4% (compressed air) respectively 9-10% (power). However, due to the high material-related impact, SLS ranges between 37.4 to 39.7 kg CO_2-eq. per kilogram of produced parts, while MJF achieves values between 29.8 and 30.1 kg CO_2-eq. in both scenarios. The influence of detailing and fusing agent in MJF is comparably low. Overall, the SLS process shows a slightly higher emission characteristic for partially filled build chambers (n=145), whereas MJF shows nearly equal results for both batch sizes.

5. Discussion and outlook

As shown in preceding research, resource and energy utilization in rapid manufacturing vary by choice of process and material handling strategies. These differences demand closer analysis of AM systems, as their number and the number machine manufacturers continues to grow [4] and it remains questionable if their wider adoption leads to energy savings in production [36]. To draw accurate conclusions, comparability to alternative manufacturing technologies such as injection molding needs to become more comprehensive. To meet this demand and generate further insights into the young MJF process, we proposed an approach to model energy and resource utilization for PBF systems. In the context of the existing literature, the generated results regarding energy consumption in the SLS process match with the results proposed by Baumers et al., reporting around 100 kWh for a full print on a comparable machine. However, packing density is likely lower, so a higher specific energy of 66 kWh/kg of sintered material is reported. Taking the broader research landscape into account, the results presented here fall into the range of reported values between 14.5 and 66 kWh/kg [19–23]. Looking at full LCA results, Kellens et al. presented similar values as presented in 4.2, with material accounting for more than 41 % of the overall impact. However, from our point of view, earlier studies tend to underestimate the primary energy demand for the manufacture of PA12 due to low data availabilty and substitution with PA6 life-cycle inventories [24, 37, 38]. Later, Devaux and Pees from the powder manufacturer Arkema [33] published data, indicating that the impact of PA12 is significantly higher (207 MJ/kg and 6.9 kg CO_2-eq.), which leads to a comparably higher contribution of

sintered and lost PA12 material to the GWP and CED results in this paper. Researchers also underlined the influence of powder recyclability for improvements in resource efficiency [21, 37], which is demonstrated by the direct comparison of the results for SLS and MJF in this paper, where MJF benefits from its high powder reusability. Concerning use of electricity, the results indicate that MJF is comparably less efficient, what might be caused by unused insulation potentials and the high air-flow through the machine. Results also indicate that MJF is less sensitive to partial builds, whereas energy and resource utilization in SLS intensifies with partial builds.

To enhance accuracy and transferability of the proposed model, more data is needed on which automated evaluation frameworks can be built, e.g. through machine learning techniques. Also we found access to job metadata on the machines very restrictive, which prevents researchers from developing accurate models and proposing further potentials for improvements in resource and energy utilization.

References

[1] M. Wiese, S. Thiede, C. Herrmann, Rapid manufacturing of automotive polymer series parts: A systematic review of processes, materials and challenges, Additive Manufacturing 36.

[2] D. Chen, S. Heyer, S. Ibbotson, K. Salonitis, J. G. Steingrímsson, S. Thiede, Direct digital manufacturing: definition, evolution, and sustainability implications, Journal of Cleaner Production 107 (2015) 615–625.

[3] C. Tuck, R. J. M. Hague, N. Burns, Rapid manufacturing: Impact on supply chain methodologies and practice, International Journal of Services and Operations Management 3 (1) (2007) 1–22.

[4] S. Karevska, G. Steinberg, A. Müller, R. Wienken, C. Kilger, D. Krauss, 3D printing: hype or game changer? A Global EY Report (2019).

[5] A. Gebhardt, J. Kessler, L. Thurn, 3D printing: Understanding additive manufacturing, 2nd Edition, Hanser Publications, Cincinnati Ohio, 2019.

[6] D. Rejeski, F. Zhao, Y. Huang, Research needs and recommendations on environmental implications of additive manufacturing, Additive Manufacturing 19 (2018) 21–28.

[7] T. Peng, K. Kellens, R. Tang, C. Chen, G. Chen, Sustainability of additive manufacturing: An overview on its energy demand and environmental impact, Additive Manufacturing 21 (2018) 694–704.

[8] S. Ford, M. Despeisse, Additive manufacturing and sustainability: an exploratory study of the advantages and challenges, Journal of Cleaner Production 137 (2016) 1573–1587.

[9] R. Sreenivasan, A. Goel, D. L. Bourell, Sustainability issues in laser-based additive manufacturing, Physics Procedia 5 (2010) 81–90.

[10] Deutsches Institut für Normung e.V., DIN EN ISO/ASTM 52900:2018: Additive manufacturing - General principles - Terminology (2018).

[11] S. C. Ligon, R. Liska, J. Stampfl, M. Gurr, R. Mülhaupt, Polymers for 3D Printing and Customized Additive Manufacturing, Chemical reviews 117 (15) (2017) 10212–10290.

[12] S. G. Rudisill, A. S. Kabalnov, K. A. Prasad, S. Ganapathiappan, J. Wright, V. Kasperchick, Three-dimensional (3D) printing: US2018/0272602A1 (2018).

[13] H. J. O'Connor, A. N. Dickson, D. P. Dowling, Evaluation of the mechanical performance of polymer parts fabricated using a production scale multi jet fusion printing process, Additive Manufacturing 22 (2018) 381–387.

[14] D. Tasch, M. Schagerl, B. Wazel, G. Wallner, Impact behavior and fractography of additively manufactured polymers: Laser sintering, multijet fusion, and hot lithography, Additive Manufacturing 29 (2019) 100816.

[15] F. Sillani, R. G. Kleijnen, M. Vetterli, M. Schmid, K. Wegener, Selective laser sintering and multi jet fusion: Process-induced modification of the raw materials and analyses of parts performance, Additive Manufacturing 27 (2019) 32–41.

[16] G. Craft, J. Nussbaum, N. Crane, J. P. Harmon, Impact of extended sintering times on mechanical properties in PA-12 parts produced by powderbed fusion processes, Additive Manufacturing 22 (2018) 800–806.

[17] I. Gibson, D. W. Rosen, B. Stucker, Additive Manufacturing Technologies: Rapid Prototyping to Direct Digital Manufacturing, Boston, MA, 2010.

[18] A. Emamjomeh, K. A. Prasad, M. A. Novick, E. Montei Fung, Detailing agent for three-dimensional (3D) printing: US2018/0022923A1 (2018).

[19] R. Sreenivasan, D. Bourell, Sustainability Study in Selective Laser Sintering – An Energy Perspective, Proceedings of the 20th Solid FreeformFabrication Symposium (2009) 3–5.

[20] M. Baumers, C. Tuck, D. L. Bourell, R. Sreenivasan, R. Hague, Sustainability of additive manufacturing: measuring the energy consumption of the laser sintering process, Proceedings of the Institution of Mechanical Engineers, Part B: Journal of Engineering Manufacture 225 (12) (2011) 2228–2239.

[21] J. Bertling, J. Blömer, M. Rechberger, S. Schreiner, DDM – An Approach Towards Sustainable Production?, Young 35 (32) (2014) 30–35.

[22] K. Kellens, E. Yasa, Renaldi, W. Dewulf, J. P. Kruth, J. R. Duflou, Energy and resource efficiency of SLS/SLM processes, 22nd Annual International Solid Freeform Fabrication Symposium - An Additive Manufacturing Conference, SFF 2011 (2011) 1–16.

[23] K. Kellens, R. Mertens, D. Paraskevas, W. Dewulf, J. R. Duflou, Environmental Impact of Additive Manufacturing Processes: Does AM Contribute to a More Sustainable Way of Part Manufacturing?, Procedia CIRP 61 (2017) 582–587.

[24] V. Tagliaferri, F. Trovalusci, S. Guarino, S. Venettacci, Environmental and Economic Analysis of FDM, SLS and MJF Additive Manufacturing Technologies, Materials 12 (24).

[25] M. A. Jackson, A. van Asten, J. D. Morrow, S. Min, F. E. Pfefferkorn, Energy Consumption Model for Additive-Subtractive Manufacturing Processes with Case Study, International Journal of Precision Engineering and Manufacturing-Green Technology 5 (4) (2018) 459–466.

[26] M. Yosofi, O. Kerbrat, P. Mognol, Energy and material flow modelling of additive manufacturing processes, Virtual and Physical Prototyping 13 (2) (2018) 83–96.

[27] Verein Deutscher Ingenieure, VDI 3633-1: Simulation of systems in materials handling, logistic and production (2014).

[28] A. Borshchev, A. Filippov, From System Dynamics and Discrete Event to Practical Agent Based Modeling: Reasons, Techniques, Tools, The 22nd International Conference of the System Dynamics Society.

[29] S. Thiede, Energy efficiency in manufacturing systems, Sustainable production, life cycle engineering and management, Springer, Berlin, 2012.

[30] A. Dietmair, A. Verl, A generic energy consumption model for decision making and energy efficiency optimisation in manufacturing, International Journal of Sustainable Engineering 2 (2) (2009) 123–133.

[31] S. Mousavi, S. Thiede, W. Li, S. Kara, C. Herrmann, An integrated approach for improving energy efficiency of manufacturing process chains, International Journal of Sustainable Engineering 9 (1) (2015) 11–24.

[32] M. Schönemann, Multiscale Simulation Approach for Battery Production Systems, Sustainable production, life cycle engineering and management, Springer International Publishing, Cham, 2017.

[33] J.-F. Devaux, G. Lê, B. Pees, Application of eco-profile methodology to polyamide 11.

[34] P. Icha, G. Kuhs, Entwicklung der spezifischen Kohlendioxid-Emissionen des deutschen Strommix in den Jahren 1990 - 2019, Dessau-Roßlau (2020).

[35] M. B. London, Cradle-to-Gate Life Cycle Assessment of Multi-Jet Fusion 3D Printing (2020).

[36] L. A. Verhoef, B. W. Budde, C. Chockalingam, B. García Nodar, A. J. van Wijk, The effect of additive manufacturing on global energy demand: An assessment using a bottom-up approach, Energy Policy 112 (2018) 349–360.

[37] C. Telenko, C. Seepersad, Assessing Energy Requirements and Material Flows of Selective Laser Sintering of Nylon Parts.

[38] K. Kellens, R. Renaldi, W. Dewulf, J.-P. Kruth, J. Duflou, Environmental impact modeling of selective laser sintering processes, Rapid Prototyping Journal 20 (2014) 459–470.